Thermo-Hydro-Mechanical Process

Tianyuan Zheng, Thomas Nagel

8th September 2017

1 Governing equations

The numerical analysis of multi-field problems in porous media is an important task for different geo-engineering subjects (e.g., geothermal energy, oil and gas reservoirs, energy storage and nuclear waste management). In particular, the coupling between heat transport and biphasic consolidation in saturated porous media is of high practical relevance.

To simulate the thermo-hydro-mechanical processes, the basic set of governing equations is given as:

- Mass (volume) balance

$$\text{div}\left[(\mathbf{u}_{\text{S}})'_{\text{S}} + \phi_{\text{F}}\mathbf{w}_{\text{FS}}\right] = \underbrace{\beta_{\text{T}}^{\text{eff}}T'_{\text{S}}}_{\text{first term}} + \underbrace{\phi_{\text{F}}\beta_{\text{TF}}\text{grad}\,T \cdot \mathbf{w}_{\text{FS}}}_{\text{second term}} \tag{1}$$

with $\phi_{\text{F}}\mathbf{w}_{\text{FS}} = -\boldsymbol{\kappa}_{\text{F}}/\mu_{\text{FR}}\left[\text{grad}\,p - \varrho_{\text{FR}}\boldsymbol{g}\right]$ and $\beta_{\text{T}}^{\text{eff}} = \phi_{\text{F}}\beta_{\text{TF}} + 3(1-\phi_{\text{F}})\alpha_{\text{TS}}$

- Momentum balance

$$\text{div}\left[\boldsymbol{\sigma}_{\text{S}}^{\text{E}} - \alpha_{\text{B}}p\boldsymbol{I}\right] + \varrho^{\text{eff}}\boldsymbol{g} = \boldsymbol{0} \tag{2}$$

with $\boldsymbol{\sigma}_{\text{S}}^{\text{E}} = \boldsymbol{\mathcal{C}} : (\boldsymbol{\epsilon} - \boldsymbol{\epsilon}_{\text{th}})$ and $\boldsymbol{\epsilon}_{\text{th}} = \boldsymbol{\alpha}_{\text{TS}}\Delta T$

- Energy balance

$$(\varrho c_p)^{\text{eff}}\frac{\partial T}{\partial t} + \phi_{\text{F}}\varrho_{\text{FR}}c_{p\text{F}}\text{grad}\,T \cdot \mathbf{w}_{\text{FS}} - \text{div}\left[\boldsymbol{\lambda}^{\text{eff}}\text{grad}\,T\right] \tag{3}$$

where α_{TS} is the linear coefficient of thermal expansion of the solid phase, β_{TF} is the volumetric coefficient of thermal expansion of the fluid phase. ϕ_{F} is the porosity. $\boldsymbol{\kappa}_{\text{F}}$ is the intrinsic permeability, μ_{FR} is the viscosity, α_{B} is the Biot coefficient, $\boldsymbol{\sigma}_{\text{S}}^{\text{E}}$ are the effective Cauchy stresses, T is the absolute temperature, p is the pore pressure, $\boldsymbol{\lambda}$ the heat conductivity and $(\bullet)'_{\alpha}$ denotes a material time derivative following the motion of the αth constituent.

In OGS-6, a model is available in which the three governing equations are assembled and solved monolithically. Different constitutive relations (e.g. elasto-plasticity, visco-elasticity) can be used to describe the material behaviour of the porous solid. For initial verification, the case of a linearly elastic solid matrix is considered here. Three numerical benchmarks were performed to verify the numerical results of thermo-hydro-mechanical process with analytical solutions. A homogeneous square model, a bi-material beam model and a point heat source consolidation model were set up for the verification.
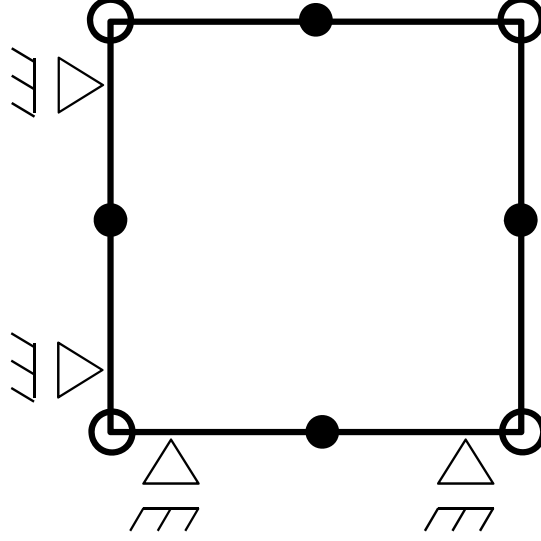
Figure 1: 2D domain and FE mesh. Square 1.0×1.0 mm; 10×10 elements

Homogeneous square model

In this case, an axisymmetric homogeneous domain (see Fig. 1) was set up with the length of $1\,\mathrm{mm}$. The whole domain was heated up from the left boundary from $273.15\,\mathrm{K}$ to $353.15\,\mathrm{K}$ and the liquid was sealed in the area from the surrounding Neumann no flow boundary. After $10000\,\mathrm{s}$, the result of the numerical solution reached steady state with homogeneous pressure of $0.1042\,\mathrm{MPa}$. Then the analytical solution of the fluid pressure created by volume expansion (see Eq. 8)is derived through the definition of general volumetric thermal expansion coefficient.

$$\beta_{\mathrm{TM}} = \frac{1}{V_{\mathrm{S}} + V_{\mathrm{F}}} \left(\frac{\partial V_{\mathrm{S}}}{\partial T} + \frac{\partial V_{\mathrm{F}}}{\partial T} \right) \tag{4}$$

with

$$
\begin{aligned}
\beta_{\mathrm{TS}} &= \frac{1}{V_{\mathrm{S}}} \left(\frac{\partial V_{\mathrm{S}}}{\partial T} \right) \\
\beta_{\mathrm{TF}} &= \frac{1}{V_{\mathrm{F}}} \left(\frac{\partial V_{\mathrm{F}}}{\partial T} \right) \\
\phi_{\mathrm{S}} &= \frac{V_{\mathrm{S}}}{V_{\mathrm{S}} + V_{\mathrm{F}}} \\
\phi_{\mathrm{F}} &= \frac{V_{\mathrm{F}}}{V_{\mathrm{S}} + V_{\mathrm{F}}}
\end{aligned}
\tag{5}
$$

In which $V_{\mathrm{S}}, V_{\mathrm{F}}$ represent the original volume of the solid phase and the fluid phase. β_{TS} and β_{TF} are the volumetric coefficient of thermal expansion of the solid phase and the fluid phase, where $\beta_{\mathrm{TS}} = 3\alpha_{\mathrm{TS}}$. ϕ_{S} and ϕ_{F} are the volume fractions of the solid phase and fluid phase.

With the modification of Eq. 4, the effective volumetric coefficient of thermal

expansion with respect to volume fraction and volumetric thermal expansion of each phase can be written as:

$$\beta_{TM} = \phi_S \beta_{TS} + \phi_F \beta_{TF} \tag{6}$$

Then the volumetric strain can be obtained according to the effective volumetric coefficient of thermal expansion and the temperature difference:

$$e_M = \beta_{TM} \triangle T \tag{7}$$

$$\begin{aligned} p &= -K_S(e_M - e^{th}) \\ &= -K_S \phi_F(\beta_{TF} - \beta_{TS})\triangle T \end{aligned} \tag{8}$$

where $e^{th} = \beta_{TS}\triangle T$. Using the analytical solution, the steady state pressure in the whole domain is $0.1042\,\text{MPa}$ with Young's Modulus of $21\,\text{MPa}$, Possion's ratio of 0.3, porosity of 0.4, volumetric thermal expansion coefficient of 2.07×10^{-4} for fluid and linear thermal expansion coefficient of 0.7×10^{-5} for solid. The numerical solution used newton-rapson method for nonlinear solver with tolerance of 10^{-7}, 10^{-5}, 10^{-5}, 10^{-5} for primary variables and BiCGSTAB for the linear solver. The numerical solution reaches steady state within $10000\,\text{s}$ and equals $0.1042\,\text{MPa}$ which fits very well with the analytical solution.

Bi-material beam model

In many application, different material domains with contrasting properties are adjacent to each other. This can pose numerical difficulties and model accuracy needs to be tested before application. For this purpose, a composite material composed of a cylindrical core and an annular domain of a different material were modelled as an axisymmetric domain with three materials was set up as illustrated in Fig. 2. The third material is the interface between the two material domains by which we control the mechanical and hydraulic connectivity of the two adjacent domains. The relationship of the different properties of the composite beam was set up as follows:

Case 1 (sealed test):

$$E_1 = 2E_3$$
$$\nu_1 = \nu_2 = \nu_3$$
$$\alpha_{TS1} = \frac{1}{2}\alpha_{TS3}$$
$$\boldsymbol{\kappa}_1 = \boldsymbol{\kappa}_3$$
$$E_2 = \frac{1}{100}E_3$$
$$\alpha_{TS2} = \frac{1}{2}\alpha_{TS3}$$
$$\boldsymbol{\kappa}_2 \approx 0$$

Case 2 (unsealed test):

$$E_1 = 2E_3$$
$$\nu_1 = \nu_2 = \nu_3$$
$$\alpha_{TS1} = \frac{1}{2}\alpha_{TS3}$$
$$\boldsymbol{\kappa}_1 = \boldsymbol{\kappa}_3$$
$$E_2 = \frac{1}{100}E_3$$
$$\alpha_{TS2} = \frac{1}{2}\alpha_{TS3}$$
$$\boldsymbol{\kappa}_2 = \boldsymbol{\kappa}_3$$

The

porosity and the Biot coefficient of the intermediate layer were both set to 0 to block the effect of temperature and pressure on solid deformation in this region and make the interface passive.
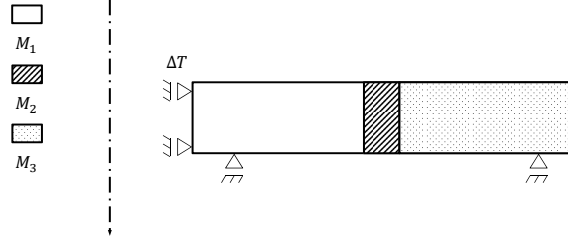
Figure 2: Bi-material domain. Texture indicates material domains 1, 2 (interface) and 3.
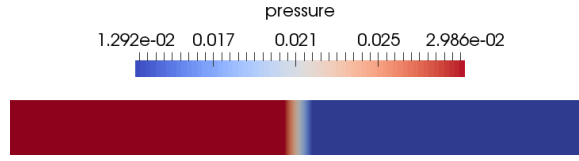

Figure 3: Pressure distribution in the composite beam

Due to the different thermal expansion coefficients between material 1 and material 3, the thermally induced volume changes of these two materials are different, which produces different fluid pressures in the materials.

For the two cases, the bottom of the model is constrained in vertical direction and the left side is constrained in horizontal direction. Temperature of $363.15\,\mathrm{K}$ is applied to the left side of the domain. The initial temperature of the whole area is set to $283.15\,\mathrm{K}$. For both case 1 and case 2, the domain is sealed.

Case 1 would be expected to capture this feature as if the two materials were separated from each other. The impermeable intermediate layer ($\kappa_2 \approx 0$) would prevent the flow moving mass from regions of higher pressure to those of lower pressure. The thermally induced volume change in material 1 is smaller than that of material 2 which leads to $p_1 > p_3$ given an identical pore fluid. Assuming the intermediate layer allowed free expansion of the neighbouring two materials, the analytical solution for the fluid pressure in each domain is

The same solver settings were used as in the previous example. The space discretization is 927 quadratic elements and the time discretization is $10\,\mathrm{s}$ with 10 time steps.

By comparing the analytical solution of the fluid pressure in the two domains, $p_1^{\mathrm{analytical}} = 0.02604\,\mathrm{MPa}$ and $p_3^{\mathrm{analytical}} = 0.01155\,\mathrm{MPa}$ to the numerical approximation, $p_1^{\mathrm{numerical}} = 0.0298\,\mathrm{MPa}$ and $p_3^{\mathrm{numerical}} = 0.0129\,\mathrm{MPa}$, a good correspondence is found. Note that due to $\kappa_2 \approx 0 \neq 0$ fluid mass is indeed moved from one domain to the other given enough time. The simulation thus needs to take this time scale into account if hydraulic isolation is to be modelled.

Case 2 established a hydraulic connection between the two reservoirs. To estimate the average modulus of the bi-material domain, the rule of mixtures was applied. Here, $E_{\mathrm{S}} = \phi_{\mathrm{S}}^{\mathrm{S1}} E_{\mathrm{S1}} + (1 - \phi_{\mathrm{S}}^{\mathrm{S1}}) E_{\mathrm{S2}}$ served as an upper-bound (in the direction of parallel to the "springs") and $E_{\mathrm{S}} = \left(\frac{\phi_{\mathrm{S}}^{\mathrm{S1}}}{E_{\mathrm{S1}}} + \frac{1 - \phi_{\mathrm{S}}^{\mathrm{S1}}}{E_{\mathrm{S2}}} \right)^{-1}$ as a lower-bound estimate (considering springs in series). The Poisson's ratios in all
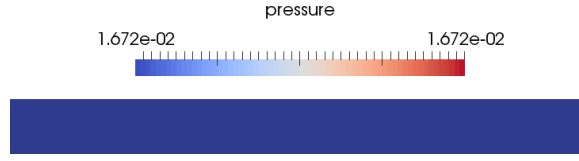
Figure 4: Pressure distribution of the unsealed test (case 2).

domains were equal $\nu_S = \nu_1 = \nu_2$, and $\phi_S^{S1} = \frac{V_{S1}}{V_{S1}+V_{S2}}$ etc.

The same method can be used to obtain the overall thermal expansion coefficient of the solid phase.

Thus, the analytical solution of the fluid pressure caused by thermal expansion evaluates to $p_{upper}^{analytical} = 0.018427499999999996\,\mathrm{MPa}$ (Arithmetic mean) and $p_{lower}^{analytical} = 0.016706666666666665\,\mathrm{MPa}$ (harmonic mean). By numerical simulation, $p^{numerical} = 0.01672\,\mathrm{MPa}$ are found which is very close to the lower bound. This is reminiscent of the fact that due to the externally unconstrained expansion and the internal fluid pressure equilibration, this set-up corresponds to the spring-in-series analogy.

Since the model setup is axisymmetric, the displacement profile along radius will be curved because of the circular geometry. If a 2D domain is considered, the displacement profile will be exact linear.

Point heat source consolidation model

When a heat source such as a canister of radioactive waste is buried in a saturated porous medium, the variation of temperature that occur will casue the pore water to expand a greater amount than the voids of the porous material. The temperature lift will thus usually be accompanied by an increase in pore pressure. If the domain is sufficiently permeable these pore pressures will dissipate. The derivation of analytical solution can be found in [1].

A 2D axisymmertic model is set up for the verification. The model domain and meshes can be found in Fig. 5. A line source is seleted to represent the injection source ($0.00204357\,\mathrm{m}$ in this case) which is located between center point of the quarter and the closest node. After the axisymmetric rotation around the vertical direction, the line source has converted into a circular source and the Neumann boundary heat flux can be thus calculated by $300/2/(\pi r^2)\mathrm{W}$. The radius of the domain is $10\,\mathrm{m}$ and the initial temperature and pore pressure are $273\,\mathrm{K}$ and $0\,\mathrm{Pa}$ respectively. The model parameters can be found in Table 1. Three different observation locations are selected for the analytical and numerical solutions ($0.25\,\mathrm{m}$, $0.5\,\mathrm{m}$ and $1\,\mathrm{m}$ from the injection source).
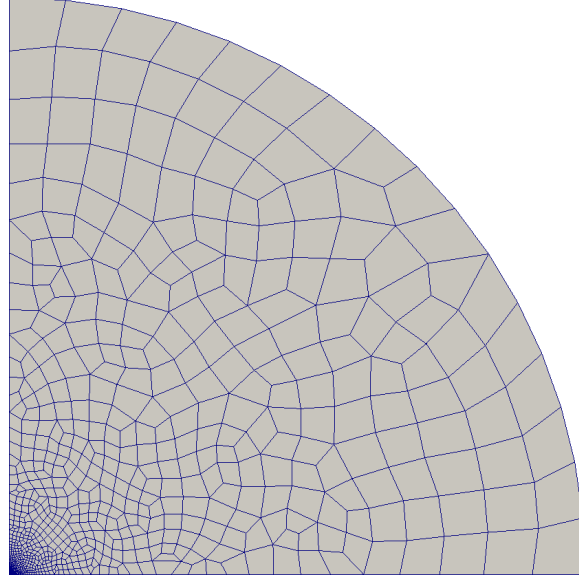
Figure 5: Mesh distribution and domain

Table 1: Parameters for the point heat source consolidation

Parameter	Value	Unit
Initial Temperature	283.15	°C
porosity	0.16	-
Water specific heat capacity	4280	J kg^{-1} K^{-1}
Water thermal conductivity	0.56	W m^{-1} K^{-1}
Water real density	1000	kg m^{-3}
Solid specific heat capacity	1000	J kg^{-1} K^{-1}
Solid thermal conductivity	1.64	W m^{-1} K^{-1}
Solid real density	2450	kg m^{-3}
Intrinsic permeability	$2 \cdot 10^{-20}$	m^2
Viscosity	$1 \cdot 10^{-3}$	Pa s
Time step size	10000	s
Young's modulus	5	GPa
Poisson's ratio	0.3	-
Biot coefficient	1	-
Fluid volumetric thermal expansion coefficient	$4 \cdot 10^{-4}$	1/K
Solid linear thermal expansion coefficient	$4.5 \cdot 10^{-5}$	1/K

From Fig. 6, Fig. 7 and Fig. 8, we can find a generally good match of the numerical solution and analytical solution. The reason that leads to the difference of analytical solution and numerical solution can be categorized into two reasons. First is that the analytical solution only considers the heat conduction process while in the fully coupled numerical model, heat advection is also included. Second is that the singularity problem can be severe in this kind of point heat source problem and will thus influence the temperature, pressure and displacement (See Figure. 9).
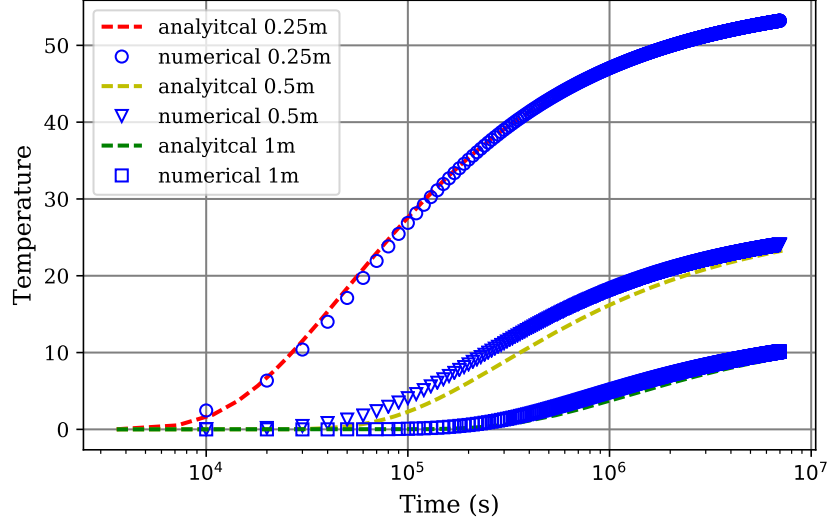
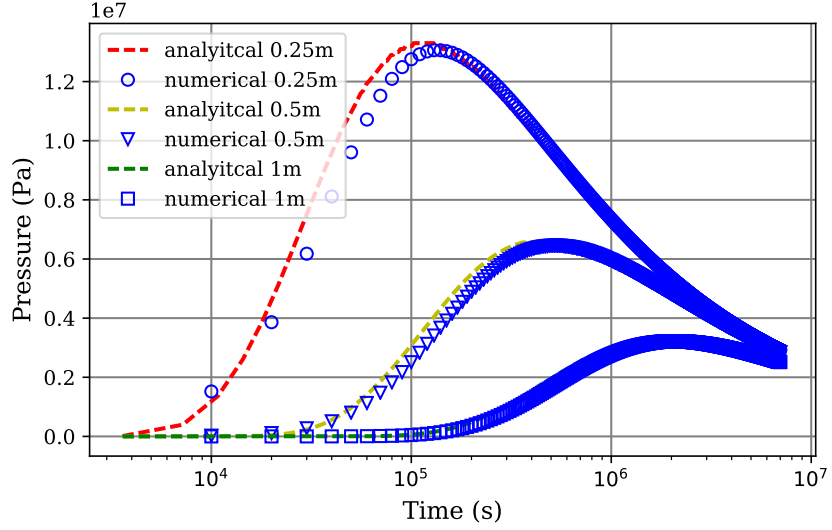Figure 6: The numerical solution compared with analytical solution (temperature)

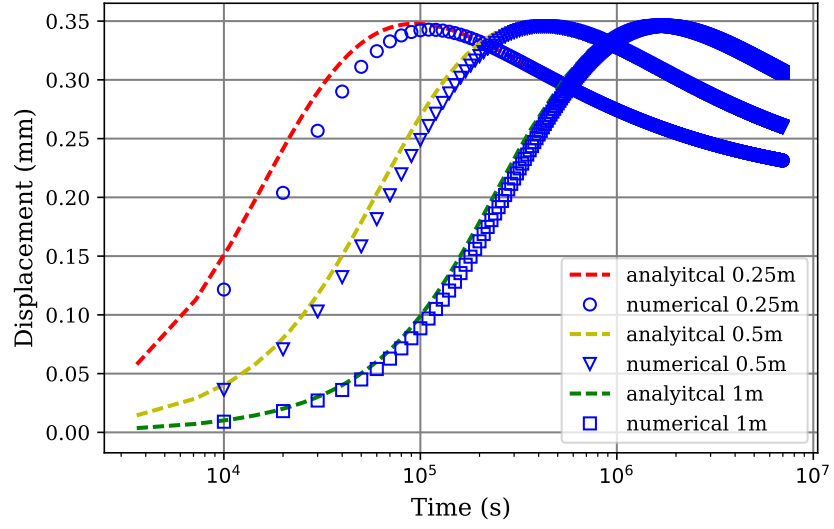Figure 7: The numerical solution compared with analytical solution (pressure)

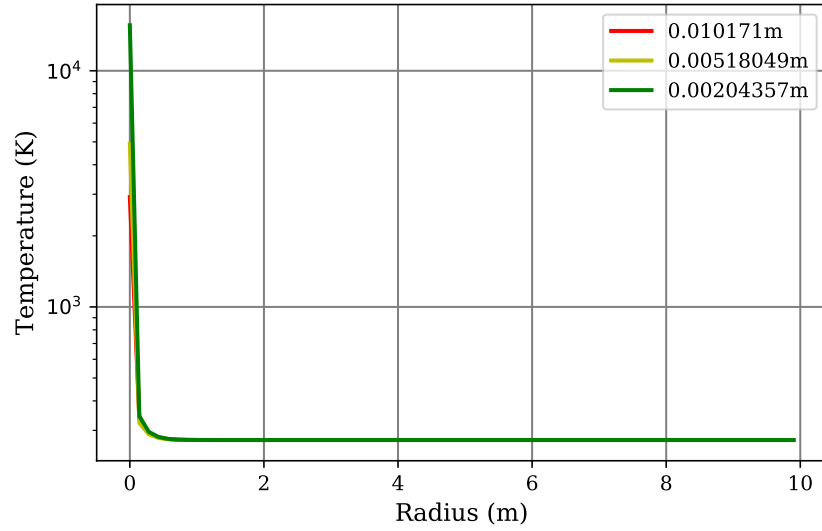Figure 8: The numerical solution compared with analytical solution (displacement)

Figure 9: The temperature profile along radius with different initial mesh size

References

[1] Olaf Kolditz, Hua Shao, Wenqing Wang, and Sebastian Bauer. Thermo-hydro-mechanical-chemical processes in fractured porous media: modelling and benchmarking. Springer, 2016.